Local Current Injector System for Nonsolenoidal Startup in a Low Aspect Ratio Tokamak

R. Fonck[1], M. Bongard[1], E. Hinson[1], B. Lewicki[1], A. Redd[1], and G. Winz[1]

[1]University of Wisconsin – Madison, Madison, WI, USA

Email contact of main author: rjfonck@wisc.edu

Abstract: Helicity injection from localized current sources in the plasma periphery of an ultralow aspect ratio spherical tokamak have produced plasma currents up to 0.15 MA with ~ 4 kA injected, and the resulting plasmas provide stable target plasmas for further current drive. This startup technique requires the development of robust, high current density sources (~ 1 kA/cm^2) that can exist in the plasma scrapeoff region during plasma initiation, growth, and possibly sustainment. An integrated assembly of active arc plasma sources and a passive electrode emitter is under development for this application to MA-class spherical tokamak applications. Compact arc plasma current sources are used for initial current injection along vacuum field lines to produce a tokamak-like plasma through null formation and Taylor relaxation. Further current growth is realized through helicity injection from these arc sources or passive electrodes in the plasma edge region. Use of passive metallic electrodes can greatly simplify the design and allow for higher injected currents to optimize the resulting plasma current. The compact, active arc sources provide an extracted current stream that appears to be governed by a double layer sheath at the arc exit region. At voltages greater than eV/kT ~ 10 and high currents, the extracted current scales as $V^{1/2}$, presumably due to the Alfven-Lawson current limit for electrons. The arc source and electrode structures are isolated from the edge plasma by a local BN limiter and nearby scraper limiter assembly. This startup approach places minimal demands on machine design.

1. Introduction

Development of scalable technology to start a current channel without solenoid induction will strongly benefit the spherical tokamak and possibly standard tokamaks. In the Pegasus Toroidal Experiment [1], relatively small, high-density current sources are placed in the plasma periphery to drive current via local helicity injection. Pegasus is an extremely low aspect ratio spherical tokamak, with major parameters R = 0.25 - 0.45 m, A = 1.1 – 1.3, elongation = 1 - 3, $I_p \sim 0.2$ MA, $B_T < 0.2$ T, $I_N \leq 14$, and $l_i \leq 0.5$. This paper describes the design status and understanding of the current sources needed to implement this novel startup technique.

Local current sources in the plasma periphery region can inject magnetic helicity and drive toroidal current, thereby creating a spherical tokamak plasma without using an ohmic solenoid [2,3]. Driving current along an open helical magnetic field created by vacuum toroidal and vertical external fields initiates the discharge. Spontaneous relaxation through MHD turbulence to a tokamak-like state occurs when the injected force-free helical current perturbs the vacuum field enough to create a local poloidal null [3]. The current sources continue to reside in the ensuing tokamak edge region and inject helicity in order to grow the plasma to high I_p. Once a tokamak-like discharge is formed, it is grown by continuing helicity input to produce a net I_p compatible with helicity balance and magnetic relaxation constraints. A stable decaying tokamak plasma forms when the external edge current drive is terminated.

The peripheral current sources can be located anywhere from the low field side midplane to the inboard divertor region [4], as indicated in Figure 1. The choice depends on access constraints, plasma control capabilities, and the desired amount of poloidal field induction.

2. Current Injector Design Requirements

Injected helicity is converted to helicity in the tokamak plasma, and that helicity is mainly lost though resistive dissipation. To sustain a tokamak-like plasma of current I_p, the total effective loop voltage provided by helicity injection and poloidal field induction is required to equal the loop voltage for an equivalent inductively driven tokamak plasma at I_p. The achievable current is limited by helicity injection and confinement properties to:

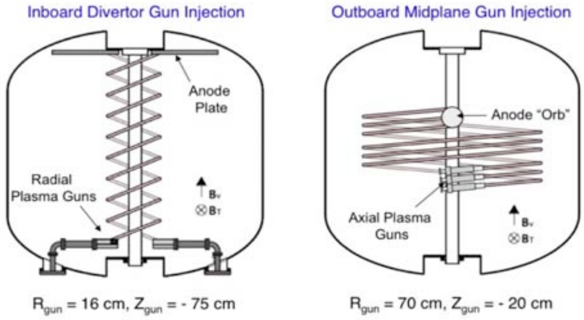

Fig. 1. Plasma gun geometries. (a) Divertor; (b) Midplane configuration.

$$I_p \leq \frac{1}{2\pi\langle\eta\rangle}\left(\frac{A_p V_{loop}}{R_0} + \frac{A_{inj} V_{inj}}{R_{inj}}\right), \tag{1}$$

where A_p is the plasma cross-section, η is the plasma resistivity, A_{inj} is the total area of the emitting electron source normal to the local field, R_{inj} is the major radius of the current source, and V_{inj} is the injector bias potential drop along the field lines. Physically, the first term is inductive drive from external poloidal field variations; the second term is the DC helicity injection drive. The maximum I_p allowed by helicity balance is inversely related to resistive dissipation, and thus strongly related to T_e. Generally, high I_p operation requires high V_{inj} for a given injector system and plasma geometry.

Helicity injection current drive relies on the relaxation of unstable plasma to the lowest energy state (the "Taylor" state) via non-axisymmetric magnetic perturbations [5]. This Taylor relaxation process imposes an upper limit on the achievable I_p for a given injector. For systems with edge current drive, the maximum I_p is set by the injector properties, edge conditions, and discharge geometry. Assuming that current and field are distributed uniformly in a turbulent edge region of thickness *w*, the maximum I_p that can be achieved by relaxation is estimated by

$$I_p \leq \frac{\Phi I_{inj}}{2\pi R B_p w} \approx f_G \sqrt{\frac{\kappa \varepsilon A_p I_{TF} I_{inj}}{2\pi R_0 w}} \tag{2}$$

where B_p is the poloidal field at a location with major radius R, ε is the inverse aspect ratio, Φ is the plasma toroidal flux, I_{TF} is the total toroidal field current, and f_G is a dimensionless function of shape parameters (ε, κ, and triangularity δ). The value of f_G varies from unity, in the circular cross-section large-A limit, to ~2.5 for typical low-A, shaped plasmas. The maximum achievable I_p using point-source helicity injection is thus either this upper limit set by relaxation, or a lesser value consistent with the helicity injection rate described above. Maximizing I_p at the relaxation limit requires high injected current in a thin edge region outside the last closed flux surface.

Experiments on Pegasus up to I_p ~ 0.15 MA have shown that Equations (1) and (2) provide a first-order description of I_p generated through this non-inductive startup technique.[3]

Generally, attaining $I_p \sim 0.2–0.3$ MA in small facilities such as Pegasus or $I_p \sim 1$ MA in larger experiments such as NSTX-U requires $V_{inj} \sim 1$ kV and $I_{inj} \sim 4$ - 12 kA. These are challenging but achievable requirements for current sources fully immersed in the edge plasma region. Additional design requirements include: acceptable impurity generation during the helicity injection phase and negligible contamination of the ensuing high-performance plasma phase; careful alignment of the electron injecting surfaces with the edge plasma flux surfaces; source impedance compatible with the desired V_{inj} and I_{inj}; and flexible gas fueling capability in the source vicinity.

3. Current Injector Concepts

Experiments on Pegasus have demonstrated non-solenoidal, high-current spherical tokamak startup via localized helicity injection in the plasma scrapeoff region. High current density arc plasma sources, derived from earlier designs [6], are used for the force-free electron current injection into the vacuum field, and can be used for the continuing plasma growth phase. A schematic of this current source is shown in Fig. 2. A 2 kA washer-stack stabilized arc is drawn through a gas-fed cylindrical channel to form a plasma with $n_e > 10^{20}$ m^{-3} and $T_e \sim 10$ eV. All exposed electrode materials are Mo, while the assembly is sheathed in a boron-nitride (BN) outer shell for electrical insulation and plasma impact. BN and PEEK insulators provide internal electrical insulation and vacuum isolation. The current is extracted by biasing the arc chamber with respect to an external anode, which is magnetically connected to the plasma guns in the vacuum magnetic field. With sufficient internal arc protection, the extracted electron current, I_{inj}, depends on the local arc plasma density and $I_{inj} \geq I_{arc}$ can be achieved with sufficient gas injection into the arc channel.

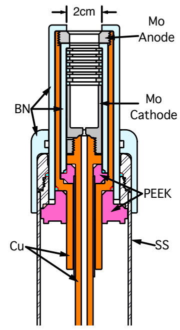

Fig. 2. Cross-section of plasma arc current source

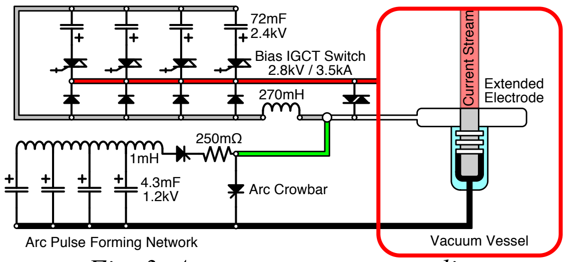

Fig. 3. Arc source power supplies

Two power systems are required for these plasma arc sources: one for the arc itself (the arc power supply), and the other for extraction of the injected current (the bias power supply). A pulse-forming network drives the internal plasma arc to provide arc currents of 1-2 kA at 100-200 V (Fig. 3). An SCR crowbar terminates the arc current on demand. The bias power supply employs a single-quadrant switch that uses four high power (2.8 kV, 3.5 kA) IGCT switches to programmable control of the injected current I_{inj}. A series inductance stabilizes the extracted current channel. An open-loop feedback controller regulates I_{inj}. The impedance of the extraction circuit depends on the arc plasma and edge plasma properties, and varies through the shot.

These point-source current injectors can be placed anywhere in the plasma boundary region, assuming sufficient port access and appropriate heat-handling capability on the source structures. To optimize net current drive, most recent experiments were performed with the plasma guns on the low-field side of the plasma, near the outer midplane, where poloidal field induction can add to the current drive available from the helicity sources. Midplane-gun discharges form at large major radius, limited on the gun and anode structures, and evolve inward until limiting on the centerstack and filling the confinement volume. Given sufficient helicity input rate, the plasma follows a trajectory governed by Eqn. 2, where I_p is limited by the Taylor relaxation limit as it grows inward, until it reaches a maximum I_p set by the net helicity injection rate (Eqn. 1) or by decoupling of the plasma from the edge current source.

Since the applied vertical field must conform to radial force balance requirements, the total V-sec available from poloidal field induction is limited, and any required remaining current drive must be supplied by helicity injection.

A disadvantage to using these arc sources is their small aperture. This follows from the definition of the helicity injection rate: $dK/dt = 2\ V_{inj}\ \Psi_{inj}$, where Ψ_{inj} is the magnetic flux intersecting the cross-sectional area of the current source. Small arc apertures require a high V_{inj} to provide a large dK/dt. Experiments on Pegasus have shown that ~ 0.15 MA is achieved with 3 arc plasma sources plus PF induction, with roughly equal contributions in effective V-sec from each. Reaching the desired goals of 0.3 MA in Pegasus and ~ 1 MA in NSTX-U requires increased helicity injection rate. A practical limit of $V_{inj} \sim 1$ kV arises in present experiments from undesired arc flashovers in the injector assembly in the presence of the edge plasma. Thus, increases in helicity input rate are more readily achieved by increasing the area of the electron emitter and I_{inj}. While a sufficiently large helicity injection rate can be provided by an increasing number of plasma arc sources, this increases the complexity of the system and requires an increasing number of discrete power supplies for the arc plasmas.

The helicity injection physics is agnostic concerning the specific source of edge current. An alternative approach to increasing the effective emission area is to employ large passive electron-emitting electrodes for current injection after the tokamak plasma is established.

After a tokamak-like plasma is formed by a minimal arc plasma source, the boundary plasma of the tokamak-like relaxed plasma is sufficiently dense to provide the environment needed to support extraction of high currents from metallic electrodes in the edge region. It is presumed that the high scrapeoff layer density provides a concentration of the sheath electric field in front of the negatively biased electrode to facilitate electron extraction through formation of localized cathode spots. This allows deployment of simple electrode structures to drive I_{inj}. The cross-sectional area of the electrodes can be significantly larger than the aperture of a plasma arc source, allowing a large helicity injection rate with a moderate bias potential V_{inj}. The shape and position of these electrodes may be tailored to provide an optimal combination of high helicity injection rate and high Taylor relaxation limit. From a technical standpoint, shaped electrodes are far easier to deploy than arrays of active plasma arc sources for the same helicity injection rate. The main helicity source is then powered by a single large bias power supply.

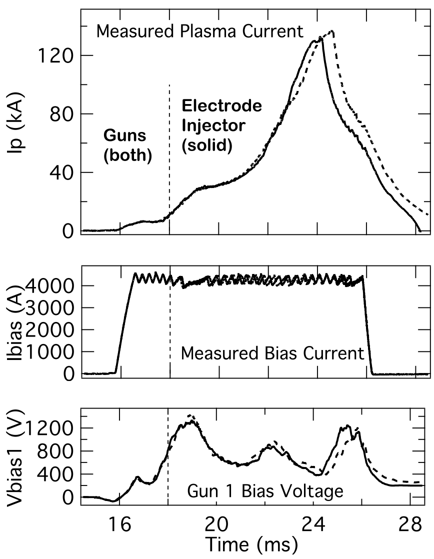

Fig. 4. Arcs off @18 ms; I_p growth by passive electrode (solid). Full-arc-on traces (dashed) shown for comparison.

Preliminary experiments to support this conjecture were conducted on Pegasus by fitting the plasma arc supplies with crowbar switches, enabling rapid extinguishment of the internal arc.[7] Initial experiments demonstrated that the extraction electrode surface can continuously source injected current through the sharp transition from active current sources to passive electrodes without an additional influx of impurities. The equivalence between injection by guns and injection by the passive electrode faces is shown by creating matched pairs of discharges, where in one discharge the arc current is switched off early in the plasma evolution. Figure 4 (from ref. 7) shows plasma current, bias current, and bias voltage for such a matched pair of discharges, where the arc current is switched off at 18 ms in the guns-as-electrodes case (solid curves). These results imply that the tokamak-like plasma is indeed providing edge conditions that support sourcing I_{inj} without an active plasma arc, and flexible electrode geometries are possible.

Hence, there is a need to explore combinations of plasma gun sources and electrodes to maximize the achievable I_p with minimal requirements on machine access, power supplies, and physical and operational complexity.

4. Active and Passive Current Injectors

To develop a current injector system that takes advantage of low-field side injection with an assist from poloidal field induction, a series of arc sources with integrated passive electrode injectors have been deployed. Figure 5 shows the evolution of varied arc-electrode source geometries tested to date. Each of these were installed in the outer plasma region, at vertical displacement of 18 cm below the plasma midplane,

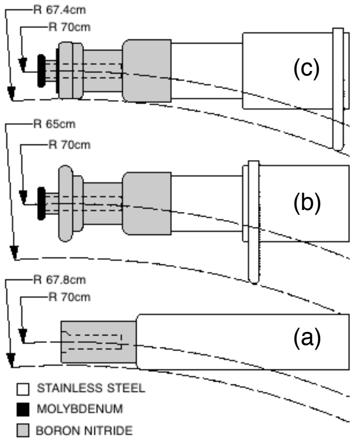

Fig. 5. Schematics of arc-source and electrode injection assemblies (top views): (a) unshielded arc sources; (b) arc source with integrated electrode; (c) arc source with integrated electrode, Mo shield plate and withdrawn scraper limiter. Curved dashed lines = magnetic flux surfaces at major radius R.

The simplest arrangement consists of 3 arc plasma sources placed vertically along the flux surface, as represented in Fig. 5(a) and shown in Fig. 6(a). Here, the arc plasma source is run continuously during the entire discharge and the arc plasma acts as the main current source. Alternatively, the extraction electrode at the plasma arc output was exposed by retraction of the BN cap to expose modest-sized electrode surfaces, as seen in Fig. 6(a). This configuration had the center of the current source 2.2 cm radially outside the filed lines contacting the innermost elements of the injector assembly. With a total I_{inj} ~ 4-5 kA, this assembly provided I_p to 0.14 MA. These discharges were limited by the available helicity injection rate, and showed considerable contamination of the plasma by N impurities, although $Z_{eff} < 3$ throughout the injection phase and dropped precipitously during an ohmically driven phase after injection was terminated.

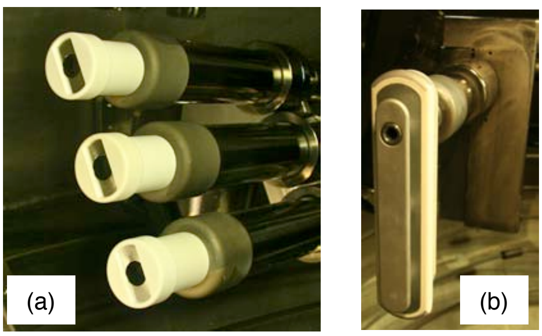

Fig. 6. (a) 3-arc source array with individual slotted electrodes; (b) arc source with large area electrode, floating Mo backing plate, and scraper limiter.

To significantly increase the available helicity input rate, a solid Mo electrode surface was installed connecting and filling the area between 3 arc sources. This is shown in Fig. 5(b). The 3 x 20 cm continuous electrode is placed in front of a BN backing plate, which acts to interrupt arc-backs from the electrode to a grounded limiter upstream from the injected current source. A later design reduced the number of plasma arc tubes to 1 from the original 3. This latter single-arc-tube plus integrated electrode assembly acts a prototypical injector geometry for a retractable local helicity injector for deployment in large-scale experiments such as NSTX-U.

The design indicated by Fig. 5(b) has two serious limitations. First, it is susceptible to micro-arcs between the electrode and the backing BN plate. These arcs do not carry significant current directly, but they do cause a significant increase in neutral gas pressure and consequent reduction of the source impedance. This is coupled with a large increase in N and B line radiation from the plasma. This leads to a precipitous drop in the V_{inj} and helicity injection rate. This arcing leads to shot irreproducibility and an unacceptably narrow operating region that does not allow high V_{inj} operation.

The arcing between the electrode and BN insulating plate is effectively eliminated by insertion of a floating Mo plate between the electrode and BN insulator, as indicated in Fig. 5(c). A photograph of the resulting single arc-source with integrated electrode assembly is shown in Fig. 6(b).

The local limiter in the injector assembly acts to scrape off local plasma in the gun region and reduce local density in front of the injector surface. Empirically, it has been found that control of the local density in the injector region is needed to provide control of the injector impedance. Initial tests were made with this limiter ~ 5 cm radially off the flux surface defined by a large local button limiter located in the upper half of the plasma. This configuration results in a significantly lower relaxation limit to the achieved plasma current where $I_p \leq 0.1$ MA rather than the previously achieved 0.15 MA even with a larger electrode area available. This suggests the effective current sheet width in the edge region (w in Eqn. 2) is determined more by local plasma conditions in the presence of the stochastic field structures in the edge region during injection than by the injector location relative to the main poloidal limiter elsewhere in the torus. Accordingly, the present working design has the electrode ~2 cm radially off the flux surface intersected by the local scraper limiter, as indicated in Fig. 5(c).

Finally, it is noted that the impedance of the current sources is quite sensitive to the gas fueling rate flowing through the arc tube and/or presented to the electrode from external gas puffing in the plasma periphery. Specifically, operation with a plasma arc source requires a significantly higher mass flow through the arc than the fueling required for pure passive electrode operation. To accommodate the need for differing fueling rates during the discharge as the injector transitions from an arc plasma source in the first few msec (to establish the tokamak discharge) to an electrode-driven growth phase, a piezo-electric programmable gas puffing valve is incorporated into the injector tube assembly directly behind the arc chamber.

Qualitative indications from VUV spectroscopy indicate that low-Z impurities from plasma impact on the BN limiting surfaces dominate in the case of the bare arc source in Fig. 5(a). Bolometric measurements suggest $Z_{eff} < 3$ in the current injection phase, and Z_{eff} drops to ~1 in an ohmically sustained plasma following the helicity startup period. The BN contamination of the plasma appears significantly reduced by the local scraper limiter in Fig. 5(b), but quantitative measurements are not yet available. Some Mo line emission is evident when operating in the passive electrode mode and with the Mo shield plate behind the main electrode, but the overall emission is still dominated by residual low-Z O and N line emission.

5. Current Injector Impedance Behaviors

Developing an understanding of the effective impedance of these current sources is needed to provide design guidance on power supply requirements for larger experiments, and inform extrapolation of this technique to other experiments.

For the case where active arc current sources are employed, the impedance of the extraction circuit depends on the arc plasma properties and edge plasma properties, and varies in time. At low current, $I_{inj} \sim V_{inj}^{3/2}$ with a perveance that is dependent on arc fueling and the length of the injector aperture's structure. In this region, space charge limited current flowing through a double layer scales as

$$I \sim \frac{n_e V^{\frac{3}{2}}}{\chi^2}, \qquad (3)$$

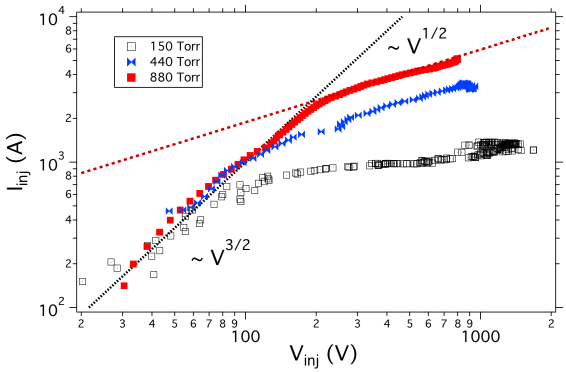

Fig. 7. I_{inj} vs. V_{inj} for different arc densities.

where χ is the double layer sheath thickness in units of the local Debye length. For estimated experimental values $I_{inj} \sim 1$ kA, $V_{inj} \sim 100$ V, $T_e \sim 10$ eV, and $n_e \sim 10^{20}$ m^{-3}, estimates of the self-consistent gap width gives $\chi \sim 15$, which is consistent with typical values expected for double layer sheaths. Assuming the arc plasma density is proportional to the injected feed gas pressure, a linear scaling of the current with density is also inferred from the data in the $V^{3/2}$ regime. Low current observations are thus consistent with a double layer sheath existing in the vicinity of the arc channel aperture.

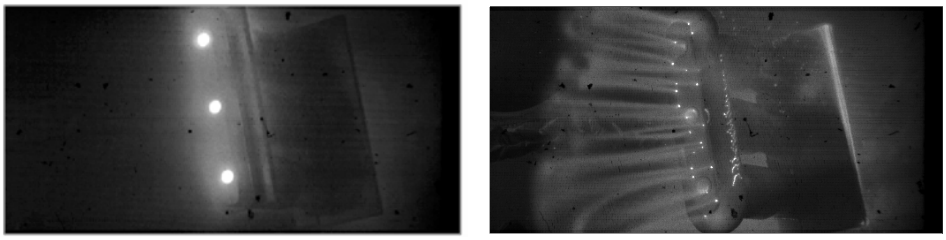

Fig. 8. Current source images during plasma growth with helicity injection. Left: plasma arc sources; Right: passive electrodes.

As V_{inj} increases to levels where $eV_{inj} > 10\ kT_e$, the extracted current I_{inj} is of the order of the Alfven current and scales as $I_{inj} \sim V_{inj}^{1/2}$ (c.f. Fig. 7). This extracted I_{inj} appears to increase linearly with the arc density. At high currents, sheath expansion or, more likely, electron beam propagation constrained by the Alfven-Lawson magnetic current limit [8] appears to dominate the impedance. Either case gives rise to a $V_{inj}^{1/2}$ scaling, and experiments are in progress to delineate the dominant mechanism. The magnetic current limit gives $I_{max} = BV^{1/2}$ where the proportionality constant depends on details of the specific model and the presumed current density profile in the extracted beam.[8,9] Typical values of B are estimated from theory to be 50 – 150, which are consistent with the attained currents in this regime.

As noted earlier, nearly identical $I_p(t)$ is observed when driven by either the current extracted from the arc source or that from a simple electrode immersed in the plasma edge once the arc current system is used to establish a background tokamak plasma. Nevertheless, the actual source of electrons is quite different. For the case of the arc discharge, electrons are extracted from the constant uniform arc column, whereas they are sourced from cathode hot spots on the active electrode surface (Fig. 8). The cathode hot spots generate randomly on the electrode surface, then tend to migrate to the electrode edge while showing characteristic rotation in the counter jxB direction. This motion of the cathode spots effectively provides the entire surface area as a current source over typical current transport times.

The impedance of the passive electrode source with multiple cathode spots is dependent on the local neutral density and presumably the local plasma density in the vicinity of the electrode. Initial current rampdown measurements indicate an $I_{inj} \sim V^{3/2}$ dependence at all currents. This suggests a similar space-charge limit mechanism at each cathode spot for the extraction of current from these local high electron density regions. For the data in Fig. 8, the approximately 25 cathode spots supply the injected current of ~ 12 kA, suggesting an average current per spot of 480 A, which is comparable to values of ~ 300 A reported for cathode spots on conditioned Mo. [10]

6. Conclusions

Non-solenoidal startup using point-source DC helicity injection has created plasmas with $I_p \sim$ 0.15 MA with $I_{inj} < 4$ kA, and current injector technologies are being developed to raise this capability to ~0.3 MA in Pegasus and project to ~1 MA nonsolenoidal startup in NSTX-U class experiments. Both active plasma current sources and passive metallic electrode injectors appear to offer viable means of providing the required high current density in the plasma scrapeoff region. Arcing and impurity generation than can occur from the placement of injector technology in the edge plasma region are being mitigated to acceptable levels by refinement of shields, limiters, and gas fueling techniques. The approach appears scalable to the MA range, and should allow the deployment of relatively small insertable hardware for startup that can be removed before a fusion plasma enters the nuclear burn phase.

This work was supported by U.S. Department of Energy Grant DE-FG02-96ER54375.

[1] GARSTKA, G. D. et al., “The upgraded Pegasus Toroidal Experiment,” Nucl. Fusion **46** (2006) S603.

[2] BATTAGLIA, D.J., et al., “Tokamak startup using point-source DC helicity injection,” Phys. Rev. Lett. **102** (2009) 225003.

[3] BATTAGLIA, D.J., et al., “Tokamak startup using outboard current injection on the Pegasus Toroidal Experiment,” Nucl. Fusion **51** (2011) 073029.

[4] Eidietis, N.W. et al., “Non-inductive production of ST plasmas with washer gun sources on the Pegasus Toroidal Experiment,” J. Fusion Energy **26** (2007) 43.

[5] TAYLOR, J. B., “Relaxation and magnetic reconnection in plasmas,” Rev. Mod. Phys. **58** (1986) 741.

[6] FIKSEL, G. et al., “High current plasma electron emitter,” Plasma Sources Sci. Technol. **5** (1996) 78.

[7] FONCK, R. J. et al., “Nonsolenoidal Startup and Plasma Stability at Near-Unity Aspect Ratio in the Pegasus Toroidal Experiment,” 23rd IAEA Fusion Energy Conference, Daejon, Korea, October 2010, no. EXS/P2-07.

[8] ALFVEN, H., “On the motion of cosmic rays in interstellar space,” Phys. Rev. 55 (1939) 425.

[9] DAVIES, J. R., “Magnetic-field-limited currents,” Phys. Rev. E 68 (2003) 037501.

[10] JUTTNER, B., “Cathode spots of electric arcs,” J. Phys. D: Appl. Phys. 34 (2001) 103.